Available online at www.sciencedirect.com

Manufacturing Letters

Manufacturing Letters 44 (2025) 325–331

53rd SME North American Manufacturing Research Conference (NAMRC 53, 2025)

Polymer metallization via cold spray: an investigation into the effects of particle hardness and morphology

Siying Chen[a], Fengfeng Zhou[a], Bailley N. Reggetz[b,c], Eun Gyung Lee[b], M. Abbas Virji[b], Aliakbar Afshari[d], Martin Byung-Guk Jun[a]*, Semih Akin[a,e]*

[a]*School of Mechanical Engineering, Purdue University, West Lafayette, IN 47907, USA*
[b]*National Institute for Occupational Safety and Health (NIOSH), Respiratory Health Division, Field Studies Branch, Morgantown, WV, USA*
[c]*West Virginia University, School of Public Health, Morgantown, WV, USA*
[d]*NIOSH, Health Effects Laboratory Division, Physical Effects Research Branch, Morgantown, WV, USA*
[e]*Department of Mechanical, Aerospace and Nuclear Engineering, Rensselaer Polytechnic Institute, Troy, NY 12180, USA*

* Corresponding author. Tel.: +1-765-494-3376; *E-mail address:* mbjun@purdue.edu
* Corresponding author. Tel.: +1-518-276-3244; *E-mail address:* akins@rpi.edu

Abstract

Metallization on polymers has captured remarkable attention across both industry and academia, facilitating the integration of unique features of polymer and metals. Particularly, direct metallization on polymers is critically important as it eliminates the need for surface activation, substrate heating, and post-processing. In this study, cold spray (CS) particle deposition was employed for direct metallization of a polymer substrate - Acrylonitrile Butadiene Styrene (ABS) - with a focus on characterizing the influence of particle (powder) hardness and their morphologies on resulting deposition. In this regard, both spherical (sp) and irregular (ir)-shaped, copper (Cu) and aluminum (Al) feedstock powders were utilized, acknowledging that Cu is intrinsically harder than Al. The metallization process on the substrate was studied in terms of microstructure, deposition efficiency, film thickness, and adhesion strength. The experimental results showed that the Cu powders achieved higher deposition efficiency (≈2.2-fold for ir-shaped, ≈2.1-fold for sp-shaped), film thickness (≈4.4-fold for ir-shaped, ≈6.4-fold for sp-shaped), and adhesion strength (≈1.9-fold for both ir- and sp-shaped) compared to the corresponding Al powders. Additionally, Cu powders exhibited lower surface porosity (24% for ir-shaped, 20% for sp-shaped), in contrast to the Al powders (51% for ir-shaped, 31% for sp-shaped). On the other hand, for both types of powders, the ir-shaped powders exhibited higher deposition efficiency (≈1.6-fold for Al and ≈1.7-fold for Cu) than the sp-shaped powders. However, irregular-shaped powders resulted in higher surface porosity (≈51% for Al-ir, ≈31% for Al-sp, ≈24% for Cu-ir, ≈20% for Cu-sp). Notably, no significant difference in adhesion strength was observed between the spherical and irregular-shaped powders. The findings elucidate the intricacies of the CS technique, contributing to functional metallization on polymeric substrates.

Peer-review under responsibility of the scientific committee of the NAMRI/SME.
Keywords: Cold spray; polymer metallization; ABS; powder hardness; powder morphology

1. Introduction

Polymers find extensive applications across various industries, including packaging [1], automotive [2], aerospace [3], sensing [4], and beyond due to their desirable properties, such as lightweight, durability, design flexibility, corrosion resistance, and so on [5]. However, their poor electrical conductivity, wear resistance, and limited thermal tolerance hinder their large-scale utilization in such applications where enhanced physical and mechanical performance is required. This challenge can be addressed by metallizing polymeric substrates, thereby achieving the unique integration of dissimilar materials (i.e., polymer + metal).

The main methods for polymer metallization include vapor deposition [6], [7], electroplating [8], electroless plating [9], and thermal spray [10]. While each method has its advantages, they often require high-temperatures, vapor phases, precursors, or strong chemicals, limiting their

Peer-review under responsibility of the scientific committee of the NAMRI/SME.

applicability for functional polymer metallization. In particular, the need for a dedicated vacuum chamber in vapor deposition and the requirement for a conductive surface in electrodeposition hinder their scalability for metallization of polymeric substrates.

Recently, the cold spray (CS) technique has gained remarkable attention in polymer metallization, as it enables one-step direct metallization of polymers under ambient conditions without requiring demanding and extensive preprocessing steps [11]. CS uses supersonic gas flow (300-1200 m/s [12]) to accelerate the micron-scale (10-100 μm [12]) metal particles (powders), which then impact a target substrate. During CS, the gas rapidly accelerates due to the pressure difference, causing a significant temperature drop and keeping the particles in a solid-state during deposition. This unique feature makes CS suitable for polymer metallization without compromising the polymers' intrinsic physical properties. Several studies have employed CS to explore the potential of this advanced manufacturing approach in polymer metallization [13–19]. Despite the advances in this field, the studies on CS-based polymer metallization considering the effects of particle hardness and morphology on resulting deposition are limited.

The main objective of this work is to investigate CS metallization (i.e., first layer build-up) on polymers by employing soft and hard particles with varying morphologies. This approach aims to enhance the understanding of the interactions between the metal powders of different hardness and morphologies and the polymer substrate during the initial layer build-up process (i.e., metallization). In this regard, aluminum (Al, soft) and copper (Cu, hard) powders, both spherical and irregular-shaped, were employed. Acrylonitrile Butadiene Styrene (ABS) was chosen as the polymer substrate due to its low cost, toughness, chemical resistance, dimensional stability, and processability, which make it suitable for a wide range of applications [20]. The resulting CS metallization was analyzed, focusing on deposition efficiency, film thickness, microstructure (i.e., porosity), and adhesion strength. The results were correlated with the observed trends to better understand the effectiveness and applicability of CS metallization on polymers.

Nomenclature

ABS	Acrylonitrile Butadiene Styrene
Al	Aluminum powder
Al-ir	Irregular shaped aluminum particles
Al-sp	Spherical shaped aluminum particles
Cu	Copper powder
Cu-ir	Irregular shaped copper particles
Cu-sp	Spherical shaped copper particles
DE	Deposition efficiency
IR	Infrared
CS	Cold spray
PFR	Powder flow rate
SEM	Scanning electron microscopy

2. Material and Methods

2.1. Materials

Al and Cu powders, both in irregular (Al-ir, Cu-ir) and spherical shapes (Al-sp, Cu-sp), were used as feedstock materials to investigate the influence of particle hardness and morphology on CS deposition characteristics. **Fig. 1** shows the scanning electron microscopy (SEM) images of the powders. The weight density of the primary materials was above 95% and the particle size distribution was the same for all powder types except for Cu-sp, which had a slightly different size distribution (**Table 1**).

ABS plates (*MSC Industrial Supply Co., Inc., Melville, NY USA*) with a thickness of 6.35 mm were used as-received without any surface-treatment. Note that the material information was obtained from the technical datasheet provided by the suppliers.

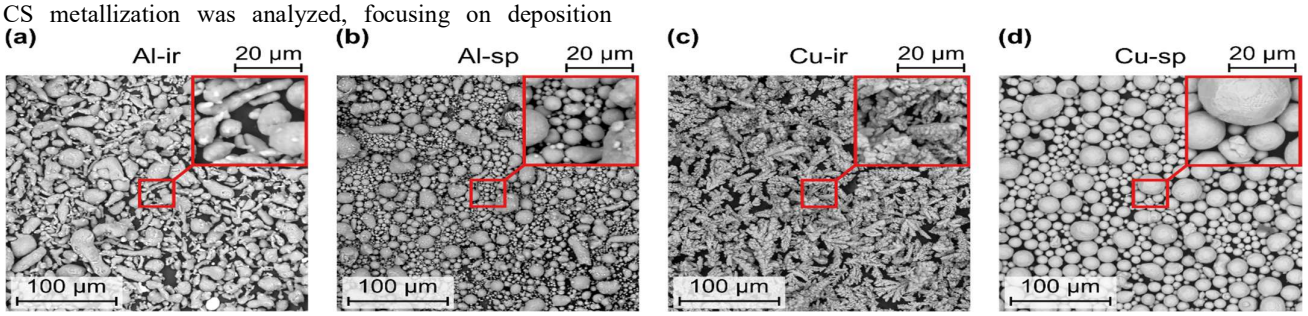

Fig. 1. SEM images of the feedstock powders: **(a)** irregular-shaped Al powders, **(b)** spherical-shaped Al powders, **(c)** irregular-shaped Cu powders, and **(d)** spherical-shaped Cu powders.

Table 1. Feedstock powders used in this study*.

Material	Supplier	Shape	Particle Size Distribution (μm)	Composition (wt%)	Hardness (HB)	Density (kg/m^3)
Aluminium (Al)	Centerline, (Windsor, Canada)	Irregular	5-45	Al ⩾ 99.5	34-37	2.7×10^3
		Spherical	5-45	Al ⩾ 95.9	72-86	
Copper (Cu)	Centerline, (Windsor, Canada)	Irregular	5-45	Cu ≥ 99.7	85-90	8.96×10^3
	Solvus Global, (Worcester, USA)	Spherical*	17-65	Cu ≥ 99.7	135	

* *Spherical Cu powder was procured from a different vendor (i.e., Solvus Global) as it was unavailable from Centerline.*

2.2. Methods

A low-pressure CS system (*CSM 108.2, Dymet, Tallinn, Estonia*) was used for the experiments. Operational settings are provided in **Table 2**. Compressed air at 0.7 MPa was used as the driving gas. The gas temperature was measured approximately 80 °C at the nozzle tip with an infrared (IR) camera (*FLIR A300, Teledyne FLIR, Wilsonville, OR USA*) under steady-state conditions. The spray gun was mounted on a robotic arm (*KR Agilus, KUKA, Augsburg, Germany*), maintaining a spray distance of 30 mm above the ABS plate. The nozzle (spray gun) moved at a constant transverse speed of 50 mm/s. Powder feeder settings were consistent for all powders. However, varying physical properties (i.e., density, hardness, morphology) resulted in different powder flow rates (see **Table 2**). It is important to note that powder flow rate in CS also depends on gas flow properties like pressure and temperature. To normalize the effects of gas phase settings, we fixed the powder feeder settings for each powder type.

Based on these observations, the powder flow rate (PFR) was determined using the gravimetric method, which involved the following sequential steps: (i) loading a known mass of powder into the feeder; (ii) operating the CS system for a fixed duration, and (iii) weighing the remaining powder in the feeder after spraying. The powder flow rate was then calculated using the following formula:

$$PFR = \frac{Initial\ powder\ mass - Remaining\ powder\ mass}{Time} \quad (1)$$

Deposition efficiency (DE), which is a critical metric in the CS process, was measured by taking the ratio between the mass of powder deposited and the mass sprayed. SEM (*PHENOM ProX, Waltham, MA USA*) was used to analyze the microstructure of the CS deposition. For each type of feedstock powder, one sample was tested, examining five locations for the surface porosity and the film thickness. The SEM images were processed using *ImageJ* software to measure the film thickness and calculate the porosity in the resulting deposition. The porosity was measured based on the surface area not covered by the metal powders. In the SEM images. These uncovered regions appeared significantly darker than the powder-deposited areas, making them easy to distinguish. The adhesion strength of the deposition was evaluated using a pull-off adhesion tester (*Elcometer 510, Elcometer Inc, Warren, MI, USA*). The details regarding the pull-off adhesion test can be found in [21]. All characterizations were conducted at room temperature with a sample size of n=3.

Table 2. Cold spray process settings.

Working gas	Air
Gas inlet gauge pressure (MPa)	0.7
Gas temperature (°C)	80 (Nozzle tip)
Powder flow rate ($g.s^{-1}$)	0.121 (Al-ir), 0.141 (Al-sp) 0.278 (Cu-ir), 0.193 (Cu-sp)
Nozzle transverse speed ($mm.s^{-1}$)	50
Nozzle stand-off distance (mm)	30

3. –Results and Discussion

It is noteworthy that the primary objective is to achieve first-layer build up (metallization) on the polymer surface. **Fig. 2 (a)** shows the DE for the powders with different morphologies on the ABS plate. CS with Cu powders resulted in higher DE (≈2.2-fold for ir-shaped, ≈2.1-fold for sp-shaped) compared to the corresponding Al powders. This is mainly due to Cu's higher density (≈ 3.3-fold) and hardness, which allows particles to achieve higher kinetic energy and penetrate deeper into soft polymer targets, ultimately leading to increased DE. **Fig.** 3 **(a)** also shows the effect of particle hardness on the DE. Since Cu particles are harder than Al particles, the DE of Cu powders is higher than that of Al powders, regardless of their morphology.

In CS, bonding on polymer substrates primarily relies on mechanical interlocking rather than metallurgical bonding [22]. As such, Cu particles achieved better mechanical interlocking, thereby increasing DE compared to Al particles (see the enclosed SEM images in **Fig. 4**). Notably, DE increased when the irregular-shaped powders were used. Specifically, Al-ir powders improved DE nearly 1.6-fold compared to Al-sp powders, and a similar trend was observed for Cu powders, with an increase of ≈ 1.7-fold. This is likely due to the higher drag coefficient of irregular-shaped particles, which facilitates a higher DE [23].

Additionally, DE can be correlated with the surface porosity of the resulting coating. **Fig. 2 (b)** shows that Cu powders led to lower surface porosity (<25%) compared to Al powders (up to 60%). The comparison in **Fig. 3 (b)** also shows that Cu powders led to lower surface porosity, independent of the powder morphology. This indicates better mechanical interlocking between Cu particles and the polymer substrate, enhancing coating integrity and strength by reducing void formation. Notably, irregularly shaped powders led to higher surface porosity regardless of powder material (**Fig. 2 (b)**, **Fig. 3 (b)**). This can be mainly attributed to: (i) packing density [24], [25], (ii) flow dynamics [26], and (iii) deformation behavior [27] of the feedstock powders with different morphology. Spherical particles can fit together more closely, leading to fewer gaps and voids compared to irregularly shaped ones [28]. They also have more predictable flow dynamics, allowing for more uniform deposition [28]. Additionally, spherical particles have a single point of contact upon impact, which leads to more uniform deformation and reduce void formation [29]. As such, spherical morphology led to a lower porosity on the as-CS surface compared to the irregular powders.

Besides, porosity formation is uneven in the CS deposition. **Fig. 4 (a)-(d)** show higher porosity near the edges due to the Gaussian distribution of the CS process [30]. The nozzle generates a particle flow with the highest velocity and concentration at the center, decreasing towards the edges. This creates a parabolic velocity profile, with maximum velocity at the center and lower velocity towards the nozzle walls, leading to a higher particle concentration in the spray center. This particle alignment plays a critical role in the thickness and quality of the resulting coatings.

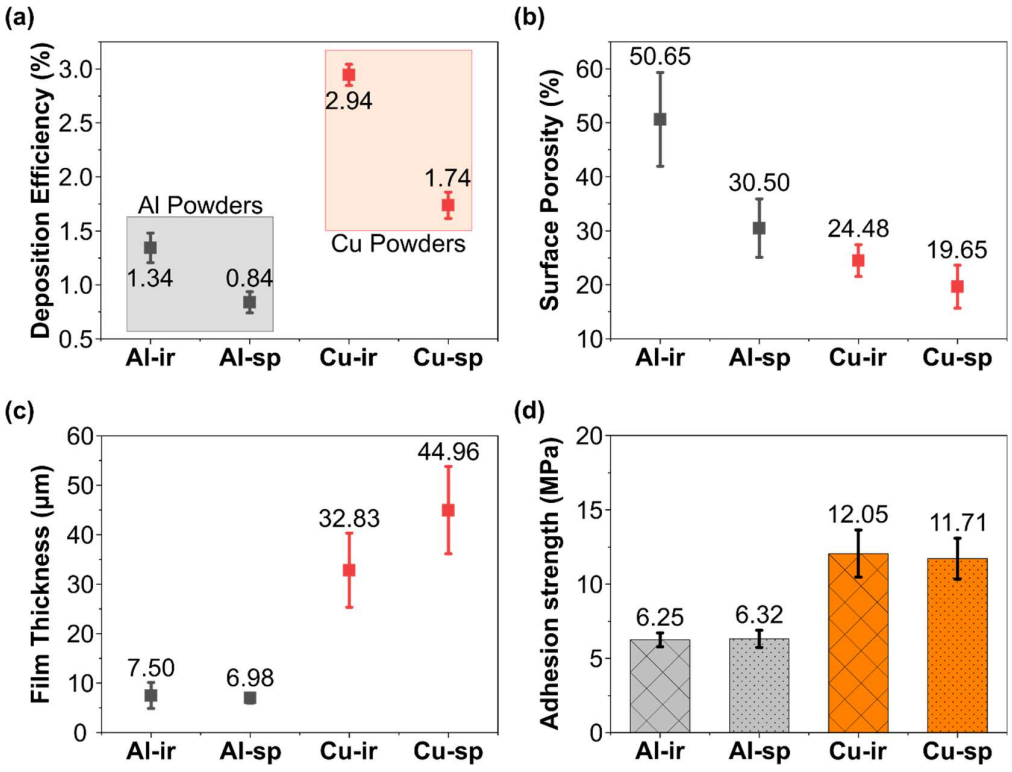

Fig. 2. **(a)** Deposition efficiency; **(b)** surface porosity; **(c)** film thickness; **(d)** adhesion strength of the resulting depositions. (Refer to Table 3 for the average magnitudes and their corresponding standard deviations).

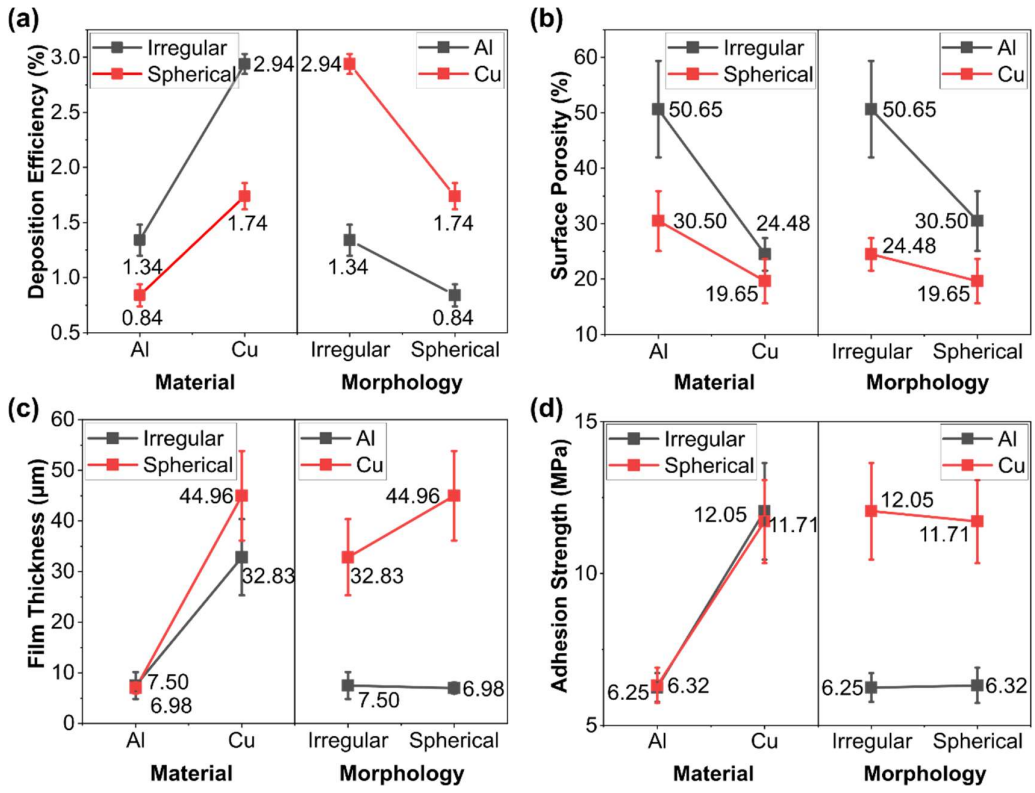

Fig. 3. Interaction effects of particle hardness and morphology with respect to **(a)** deposition efficiency, **(b)** surface porosity, **(c)** film thickness, and **(d)** adhesion strength.

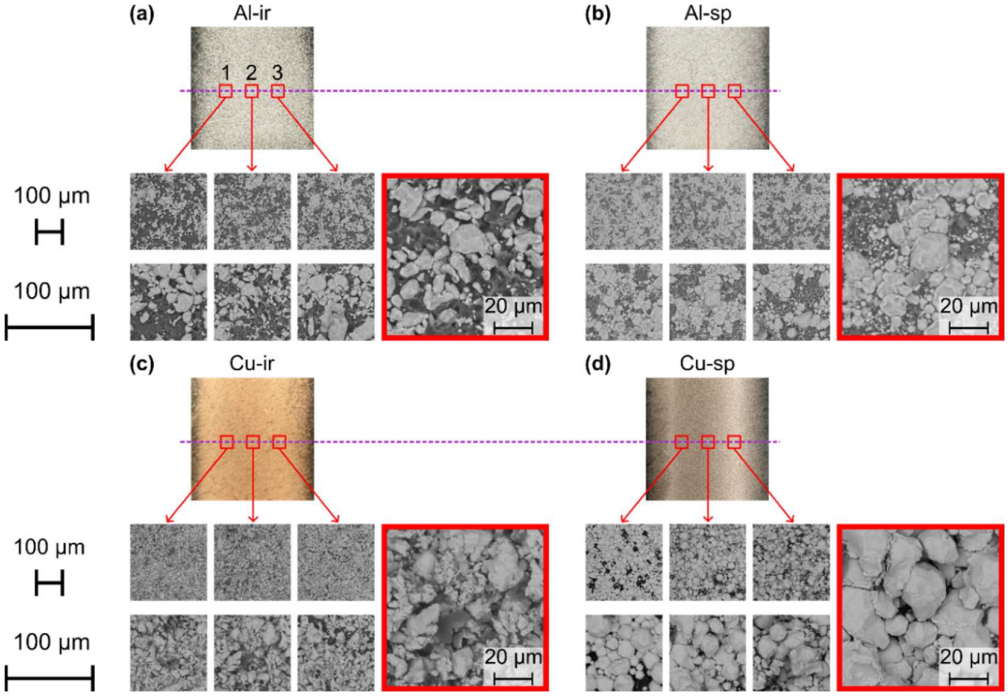

Fig. 4. Surface microstructure of the resulting metallization; **(a)** ir-shaped Al; **(b)** sp-shaped Al; **(c)** ir-shaped Cu; **(d)** sp-shaped Cu powders. The figures with red borders provide a zoomed-in view of the cross-sectional microstructure at the center of the metalized area.

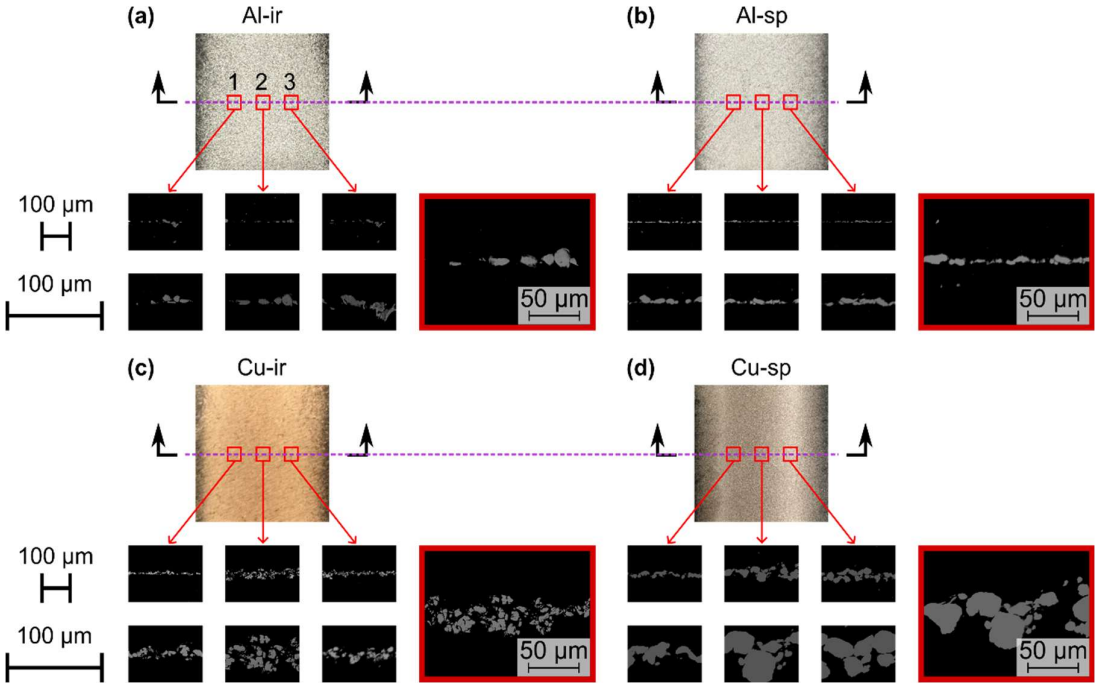

Fig. 5. Cross-section microstructure of the resulting metallization; **(a)** ir-shaped Al; **(b)** sp-shaped Al; **(c)** ir-shaped Cu; **(d)** sp-shaped Cu powders. The figures with red borders provide a zoomed-in view of the cross-sectional microstructure at the center of the metalized area.

Notably, despite higher DE for Al-ir than Al-sp powders (**Fig. 2 (a)**), both Al-ir and Al-sp resulted in similar film thickness (**Fig. 2 (c)**). Conversely, Cu-sp powders led to thicker films than Cu-ir powders. Cu powder achieved greater film thickness than Al powder regardless of the particle morphology (**Fig. 3 (c)**). This difference can be attributed to varying impingement behaviors. In detail, irregular-shaped particles, with higher drag coefficients, achieve greater impact velocities [31], but their larger contact area may hinder penetration into the polymer. Spherical particles, due to their point contact, localize impact and penetrate more effectively, thereby resulting in thicker films. This phenomenon is more clearly observed in the cross-sectional SEM images shown in **Fig. 5**, where spherical particles show better particle aggregation and reduced porosity at the polymer interface, further supporting the observations noted above.

Table 3. Summary of the findings derived from this work*.

Powder	Al-ir	Al-sp	Cu-ir	Cu-sp
Deposition efficiency (%)	1.34 ± 0.14	0.84 ± 0.1	2.94 ± 0.09	1.74 ± 0.12
Surface Porosity (%)	50.65 ± 8.7	30.5 ± 5.4	24.48 ± 2.94	19.65 ± 3.99
Film Thickness (μm)	7.5 ± 2.66	6.98 ± 1.05	32.83 ± 7.52	44.96 ± 8.84
Adhesion Strength (MPa)	6.25 ± 0.47	6.32 ± 0.58	12.05 ± 1.59	11.71 ± 1.37

* *The values represent the average magnitudes along with their corresponding standard deviations*

Overall, the results indicate that although it is feasible to deposit both Al and Cu powders onto the polymer (ABS) substrate via CS, the overall DE remains remarkably low (< 3%). Typically, the DE is lower when CS is applied to polymeric substrates compared to metal substrates [32]. Accordingly, the DE results in this study align well with the literature wherein the DE of Cu on ABS polymer was reported < 5% [33]. However, it is important to note that DE is highly dependent on CS process parameters (i.e., gas type, gas temperature, gas pressure) and kinematic factors (i.e., nozzle distance, nozzle transverse speed, and tool-path strategy). As such, the DE can be improved through optimization of these settings.

Lastly, the adhesion strength of the deposition was evaluated using the pull-off adhesion test in accordance with the ASTM D4541 standard [34]. In each test, a dolly (14.2 mm in diameter) was gradually pulled until the coating detached from the polymer surface, at which point the adhesion strength of the coating was recorded, and the results were plotted, as shown in **Fig. 2 (d)**. The Cu powders achieved remarkably higher adhesion strength (1.93-fold for irregular-shaped, 1.85-fold for spherical-shaped) compared to the Al powders, and Cu powders achieved higher adhesion strength in general regardless of the particle morphology (**Fig. 2 (d)**, **Fig. 3 (d)**). This is likely attributed to higher density and hardness of Cu as compared to Al, resulting in higher impact energy for Cu particles during the CS. This increased impact energy facilitates the impingement of the Cu particles into the polymer target, resulting in stronger mechanical interlocking. The film thickness comparison in **Fig. 2 (c)** and **Fig. 3 (c)** also confirms the deeper impingement of Cu particles compared with the Al particles. This deeper impingement leads to higher adhesion strength in Cu powders than in Al powders.

Notably, the pull-off adhesion test experiments showed no significant difference in adhesion strength between the spherical and irregular-shaped powders. This observation indicates that adhesion strength is more dependent on material properties than particle shape. The main findings of this study are summarized in **Table 3**. Notably, as-CS metallized surface exhibited promising adhesion strength, surpassing commonly used polymer metallization methods, such as air plasma spray (5.21 MPa) [35], electroless plating (5.48 MPa) [36], and vapor deposition (3.02 MPa) [6].

4. Conclusion

In this work, CS metallization on a polymer substrate was studied, focusing on the influence of particle hardness and morphology on deposition. Al and Cu powders, both in irregular and spherical shapes, were sprayed on the ABS target, acknowledging that Cu is inherently harder than Al. Key metrics of the CS process, including DE, porosity, film thickness, and adhesion strength were carefully analyzed. Key takeaways from the study are:

- The Cu powders resulted in higher DE (≈2.2-fold for irregular-shaped, ≈ 2.1-fold for spherical-shaped), greater film thickness (≈4.4-fold irregular-shaped, ≈ 6.4-fold for spherical-shaped), and lower surface porosity (24% for irregular-shaped, 20% for spherical-shaped) as compared to Al. Regardless of the particle morphology, Cu powder achieved higher DE and greater film thickness. This can be attributed to better mechanical interlocking of Cu with the polymer substrate due to its higher density and hardness.
- For the same type of powder, the irregular powders resulted in remarkably higher surface porosity compared to the spherical powders (i.e., ≈51% for Al-ir, ≈31% for Al-sp, ≈24% for Cu-ir, ≈20% for Cu-sp).
- Harder powders (Cu) led to thicker film than relatively softer powders (Al), but this trend is not consistent with powder morphology.
- Harder powders (Cu) exhibited higher adhesion strength (≈ 1.9-fold) than soft powders (Al). However, no significant difference in adhesion strength was observed between the spherical and irregular-shaped powders.

The findings of the study elucidated the intricacies of CS polymer metallization by utilizing hard (Cu) and soft (Al) particles with varying morphologies. The results revealed that Cu and Al can be successfully cold sprayed onto the polymer (ABS) target, although the DE was low (0.84-2.94%). Future work may focus on enhancing DE by utilizing low-density gases such as helium and optimizing CS process parameters and kinematic factors. Additionally, further characterization of wear resistance, thermal, and electrical properties of CS-metallized polymers using various feedstock powders can be conducted.

Declaration of Competing Interest

The authors declare that they have no competing financial interests or personal relationships that could have influenced the work reported in this paper. The findings and conclusions in this report are those of the authors and do not necessarily represent the views of the National Institute for Occupational Safety and Health, Centers for Disease Control and Prevention (NIOSH/CDC). Mention of any company or product does not constitute endorsement by NIOSH/CDC.

Funding

This project was funded internally by the National Institute for Occupational Safety and Health (NIOSH, Project CAN number: 9390KKD).

References

[1] Sangroniz A, Zhu J-B, Tang X, Etxeberria A, Chen EY-X, Sardon H. Packaging materials with desired mechanical and barrier properties and full chemical recyclability. Nat Commun 2019;10:3559. https://doi.org/10.1038/s41467-019-11525-x.

[2] Gupta P, Toksha B, Patel B, Rushiya Y, Das P, Rahaman M. Recent Developments and Research Avenues for Polymers in Electric Vehicles. The Chemical Record 2022;22:e202200186. https://doi.org/10.1002/tcr.202200186.

[3] Yadav R, Tirumali M, Wang X, Naebe M, Kandasubramanian B. Polymer composite for antistatic application in aerospace. Defence Technology 2020;16:107–18. https://doi.org/10.1016/j.dt.2019.04.008.

[4] Verma A, Gupta R, Verma AS, Kumar T. A review of composite conducting polymer-based sensors for detection of industrial waste gases. Sensors and Actuators Reports 2023;5:100143. https://doi.org/10.1016/j.snr.2023.100143.

[5] Hsissou R, Seghiri R, Benzekri Z, Hilali M, Rafik M, Elharfi A. Polymer composite materials: A comprehensive review. Composite Structures 2021;262:113640. https://doi.org/10.1016/j.compstruct.2021.113640.

[6] Fumagalli N, de Haro Sanchez JC, Bianchi CL, Turri S, Griffini G. Metallization of polypropylene substrates through surface functionalization and physical vapor deposition of chromium coatings. Surface and Coatings Technology 2024;484:130880. https://doi.org/10.1016/j.surfcoat.2024.130880.

[7] Mavukkandy MO, McBride SA, Warsinger DM, Dizge N, Hasan SW, Arafat HA. Thin film deposition techniques for polymeric membranes– A review. Journal of Membrane Science 2020;610:118258. https://doi.org/10.1016/j.memsci.2020.118258.

[8] Augustyn P, Rytlewski P, Moraczewski K, Mazurkiewicz A. A review on the direct electroplating of polymeric materials. J Mater Sci 2021;56:14881–99. https://doi.org/10.1007/s10853-021-06246-w.

[9] Suman R, Nandan D, Haleem A, Bahl S, Javaid M. Experimental study of electroless plating on acrylonitrile butadiene styrene polymer for obtaining new eco-friendly chromium-free processes. Materials Today: Proceedings 2020;28:1575–9. https://doi.org/10.1016/j.matpr.2020.04.843.

[10] A Review of Thermal Spray Metallization of Polymer-Based Structures | Journal of Thermal Spray Technology n.d. https://link.springer.com/article/10.1007/s11666-016-0415-7 (accessed May 7, 2024).

[11] King P, Yandouzi M, Jodoin B. The Physics of Cold Spray. In: Villafuerte J, editor. Modern Cold Spray: Materials, Process, and Applications, Cham: Springer International Publishing; 2015, p. 31–72. https://doi.org/10.1007/978-3-319-16772-5_2.

[12] Guo D, Kazasidis M, Hawkins A, Fan N, Leclerc Z, MacDonald D, et al. Cold Spray: Over 30 Years of Development Toward a Hot Future. J Therm Spray Tech 2022;31:866–907. https://doi.org/10.1007/s11666-022-01366-4.

[13] Rokni MR, Feng P, Widener CA, Nutt SR. Depositing Al-Based Metallic Coatings onto Polymer Substrates by Cold Spray. J Therm Spray Tech 2019;28:1699–708. https://doi.org/10.1007/s11666-019-00911-y.

[14] Che H, Liberati AC, Chu X, Chen M, Nobari A, Vo P, et al. Metallization of polymers by cold spraying with low melting point powders. Surface and Coatings Technology 2021;418:127229. https://doi.org/10.1016/j.surfcoat.2021.127229.

[15] Akin S, Lee S, Jo S, Ruzgar DG, Subramaniam K, Tsai J-T, et al. Cold spray-based rapid and scalable production of printed flexible electronics. Additive Manufacturing 2022;60:103244.

[16] Zhang T, Padayodi E, Sagot J-C, Raoelison RN. Metallization of carbon-fibre reinforced composites via a metal-epoxy biphasic sublayer and low-pressure cold spraying. Powder Technology 2023;426:118575. https://doi.org/10.1016/j.powtec.2023.118575.

[17] Akin S, Nath C, Jun MB-G. Selective Surface Metallization of 3D-Printed Polymers by Cold-Spray-Assisted Electroless Deposition. ACS Appl Electron Mater 2023;5:5164–75. https://doi.org/10.1021/acsaelm.3c00893.

[18] Ruzgar DG, Akin S, Lee S, Walsh J, Lee HH, Jeong YH, et al. Highly Flexible, Conductive, and Antibacterial Surfaces Toward Multifunctional Flexible Electronics. Int J of Precis Eng and Manuf-Green Tech 2024. https://doi.org/10.1007/s40684-024-00608-w.

[19] Tsai J-T, Akin S, Bahr DF, Jun MB-G. A predictive modeling approach for cold spray metallization on polymers. Surface and Coatings Technology 2024;483:130711. https://doi.org/10.1016/j.surfcoat.2024.130711.

[20] Ford P, Fisher J. Designing consumer electronic products for the circular economy using recycled Acrylonitrile Butadiene Styrene (ABS): A case study. Journal of Cleaner Production 2019;236:117490. https://doi.org/10.1016/j.jclepro.2019.06.321.

[21] Lee J, Akin S, Walsh JR, Jun MBG, Lee H, Shin YC. A Nitinol structure with functionally gradient pure titanium layers and hydroxyapatite over-coating for orthopedic implant applications. Prog Addit Manuf 2023. https://doi.org/10.1007/s40964-023-00500-0.

[22] Heydari Astaraee A, Colombo C, Bagherifard S. Insights on metallic particle bonding to thermoplastic polymeric substrates during cold spray. Sci Rep 2022;12:18123. https://doi.org/10.1038/s41598-022-22200-5.

[23] Alonso L, Garrido-Maneiro MA, Poza P. A study of the parameters affecting the particle velocity in cold-spray: Theoretical results and comparison with experimental data. Additive Manufacturing 2023;67:103479. https://doi.org/10.1016/j.addma.2023.103479.

[24] Stovall T, de Larrard F, Buil M. Linear packing density model of grain mixtures. Powder Technology 1986;48:1–12. https://doi.org/10.1016/0032-5910(86)80058-4.

[25] Mussatto A, Groarke R, O'Neill A, Obeidi MA, Delaure Y, Brabazon D. Influences of powder morphology and spreading parameters on the powder bed topography uniformity in powder bed fusion metal additive manufacturing. Additive Manufacturing 2021;38:101807. https://doi.org/10.1016/j.addma.2020.101807.

[26] Brika SE, Letenneur M, Dion CA, Brailovski V. Influence of particle morphology and size distribution on the powder flowability and laser powder bed fusion manufacturability of Ti-6Al-4V alloy. Additive Manufacturing 2020;31:100929. https://doi.org/10.1016/j.addma.2019.100929.

[27] Wong W, Vo P, Irissou E, Ryabinin AN, Legoux J-G, Yue S. Effect of Particle Morphology and Size Distribution on Cold-Sprayed Pure Titanium Coatings. J Therm Spray Tech 2013;22:1140–53. https://doi.org/10.1007/s11666-013-9951-6.

[28] Hussain T, Yue S, Li C-J. Characteristics of Feedstock Materials. In: Villafuerte J, editor. Modern Cold Spray: Materials, Process, and Applications, Cham: Springer International Publishing; 2015, p. 73–105. https://doi.org/10.1007/978-3-319-16772-5_3.

[29] Weiller S, Delloro F. A numerical study of pore formation mechanisms in aluminium cold spray coatings. Additive Manufacturing 2022;60:103193. https://doi.org/10.1016/j.addma.2022.103193.

[30] Klinkov SV, Kosarev VF, Shikalov VS. Influence of nozzle velocity and powder feed rate on the coating mass and deposition efficiency in cold spraying. Surface and Coatings Technology 2019;367:231–43. https://doi.org/10.1016/j.surfcoat.2019.04.004.

[31] Bhattiprolu VS, Johnson KW, Ozdemir OC, Crawford GA. Influence of feedstock powder and cold spray processing parameters on microstructure and mechanical properties of Ti-6Al-4V cold spray depositions. Surface and Coatings Technology 2018;335:1–12. https://doi.org/10.1016/j.surfcoat.2017.12.014.

[32] Liberati AC, Che H, Aghasibeig M, Yu KR, Vo P, Yue S. On the Importance of Secondary Component Properties for Cold Spray Metallization of Carbon Fiber Reinforced Polymers. J Therm Spray Tech 2022;31:159–75. https://doi.org/10.1007/s11666-022-01323-1.

[33] Che H, Chu X, Vo P, Yue S. Metallization of Various Polymers by Cold Spray. J Therm Spray Tech 2018;27:169–78. https://doi.org/10.1007/s11666-017-0663-1.

[34] Standard Test Method for Pull-Off Strength of Coatings Using Portable Adhesion Testers n.d. https://www.astm.org/d4541-22.html (accessed February 11, 2025).

[35] Guanhong S, Xiaodong H, Jiuxing J, Yue S. Parametric study of Al and Al2O3 ceramic coatings deposited by air plasma spray onto polymer substrate. Applied Surface Science 2011;257:7864–70. https://doi.org/10.1016/j.apsusc.2011.04.057.

[36] Zhang A, Wu W, Xie D. Influence of laser treatment on the adhesion force of metallized carbon fiber reinforced polymer (CFRP) composite. International Journal of Adhesion and Adhesives 2024;135:103830. https://doi.org/10.1016/j.ijadhadh.2024.103830.